Near-resonant dark optical lattice with increased occupation

Vladimir Elman and Andreas Hemmerich
Institut für Laser-Physik, Universität Hamburg, Luruper Chaussee 149, D-22761 Hamburg, Germany
(Received 26 May 2005; published 31 October 2005)

A bichromatic near-resonant dark optical lattice (DOL) with rubidium atoms is demonstrated, which provides confinement in the Lamb-Dicke regime in all spatial dimensions. We apply spatially phase-matched optical potentials for each hyperfine ground state in order to enable improved Sisyphus cooling, undisturbed by optical hyperfine pumping processes. We also explore a method to increase the occupation of the DOL. Initially 2×10^9 rubidium atoms with a temperature of 70 μK and a density of 5×10^{10} atoms/cm^3 are prepared in a magneto-optic trap (MOT) and a fraction of 5×10^7 atoms is loaded into a far detuned one-dimensional optical lattice (FOL). Subsequently, the MOT is replaced by the DOL, and the atoms become well localized within the microscopic light-shift potentials at a temperature of 10 μK with a typical density of 3×10^{11} atoms/cm^3. We then apply alternating cycles of free evolution in the FOL and cooling and trapping in the DOL, obtaining a fourfold density increase to 1.2×10^{12} atoms/cm^3—i.e., 7.5% occupation—while maintaining a temperature of 10 μK. In a final adiabatic cooling step we reduce the well depth to 75 times the single-photon recoil energy, which leads to a temperature of 2.8 μK and a phase-space density of 1.7×10^{-3}. Despite the increased density, no excess heating or collisional losses are observed.

DOI: 10.1103/PhysRevA.72.043410 PACS number(s): 32.80.Pj, 42.50.Vk

Optical lattices are regular arrays of atoms confined in the microscopic light-shift potentials of optical standing waves [1–4]. Conventional near-resonant optical lattices [denoted as bright optical lattices (BOL's) in the following] are produced by light fields detuned by a few linewidths to the red side of an atomic resonance. In this type of optical lattice atoms scatter photons at a high rate because they are located in the vicinity of the antinodes of the light field—i.e., locations where the atom-light interaction is maximal. Extensive photon scattering, however, may distort the lattice field and thus degrade the cooling and trapping efficiency. Typically, undesired repelling forces arise among the atoms [5–7] and light-induced collisions lead to atom losses [8]. As a consequence, the atomic density in BOL's is limited to values below 10^{11} atoms/cm^3, while temperatures exceed 10 μK, which corresponds to filling factors below 1% and phase-space densities below 10^{-5}. This is unfortunate because the regime of high densities, when the number of trapped atoms matches or even exceeds the number of lattice sites, is particularly interesting, since mutual interactions and quantum statistics then provide a wealth of new physics. The advent of Bose-Einstein condensates [9] has made this regime accessible in far-detuned optical lattices, where spontaneous scattering is negligible and no built-in optical cooling mechanisms exist [10,11].

An interesting approach to significantly reduce the rate of spontaneous scattering, while maintaining a built-in cooling mechanism, is the concept of dark optical lattices (DOL's) [12,13]. In contrast to BOL's, the elastic scattering contribution (predominant in BOL's) is entirely suppressed in DOL's and merely those scattering processes are maintained which are necessary to provide cooling. A typical scenario in a DOL operates as follows: the total light field can be decomposed into two polarization components such that the intensity maxima of one component coincide with the minima of the other. One of these polarization components traps the atoms in its nodes (DOL's operate with blue detuning) where photon scattering is minimal. The other polarization component, although maximal at these locations, cannot couple to the atoms there because of some radiation selection rule. Only since the atoms are not perfectly localized in the nodes of the first polarization component can residual coupling of the second component occur in the wings of the atomic wave functions. The overall photon scattering is thus reduced to those photons essential for maintaining a Sisyphus cooling process [14]. Experimentally, DOL's are formed by the interplay between a near-resonant blue-detuned light field and an external homogeneous magnetic field [12,13]. Unfortunately, in contrast to the case of BOL's, for DOL's most beam configurations yield light-shift potentials which do not provide confinement in all spatial dimensions [4], which may be the reason why experiments with DOL's admitting truly three-dimensional confinement have not yet been reported. The reduced fluorescence level in DOL's suggests that higher filling factors should be accessible as compared to BOL's. However, the loading of a DOL typically requires precooling and trapping of atoms in a magneto-optical trap (MOT) [16,17]; i.e., densities are limited by the MOT physics to values comparable to those obtained in BOL's. Hence, additional efforts are required in order to further increase the atomic density and explore the capacity of DOL's to hold such atomic samples.

In this paper we study a DOL in a truly three-dimensional (3D) configuration [cf. Fig. 1(a)], providing potential minima, which are singular points in three dimensions in contrast to earlier implementations, where the light-shift potentials formed complex surfaces [18,19] or lines [13], thereby providing escape channels for the atoms. We apply two spatially phase-matched optical potentials for each hyperfine component of the atomic ground state in order to enable optimal spatial correlations between light shifts and optical pumping rates including optical hyperfine pumping processes. This yields lower temperatures and higher vibrational ground-state occupations as compared to previous near-resonant optical lattices. Our DOL performs remarkably well in the regime of large magnetic fields. The kinetic tem-

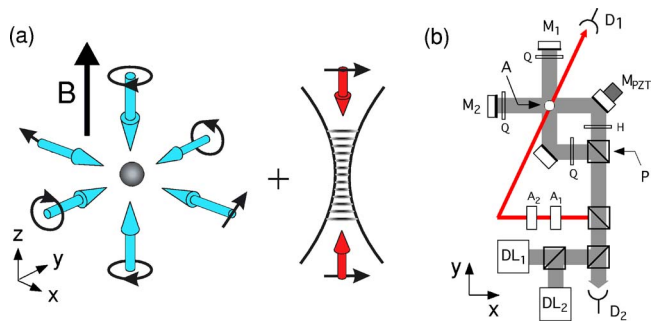

FIG. 1. (Color online) (a) Sketch of laser beam configuration of the 3D DOL (left) and FOL (right). (b) Sketch of the experimental setup for producing a 2D dark optical lattice in the xy plane. Q =quarter-wave plate, H=half-wave plate, P=polarizing beam splitter, A_i=acousto-optic modulator, M_i=mirror, M_{PZT}=piezoactuated mirror, D_i=photodetector, and DL_i=diode laser.

perature of our DOL in this regime is determined mainly by the quantum-mechanical momentum uncertainty of the vibrational ground state which is populated by 90% of the atoms for well depths above $75E_{rec}$ (E_{rec} is the recoil energy of a single 795-nm photon). We use a simple scheme, inspired by earlier work in a far-detuned lattice with cesium atoms [15], that provides us with a fourfold density increase over the initial MOT density, limited mainly by technical deficiencies of our experiment. This scheme uses an additional intense 1D far-detuned optical lattice (FOL) which is superimposed upon the 3D DOL [cf. Fig. 1(a)]. Alternating cycles of free evolution in the microscopic potentials of the FOL, cooling and trapping in the DOL, and adiabatic cooling in the DOL yield a fourfold density increase and a threefold temperature decrease. We thus obtain a density of 1.2×10^{12} atoms/cm^3—i.e., 7.5% occupation—and a temperature of 2.8 μK, yielding a phase-space density of 1.7×10^{-3}. This improves typical phase-space densities around 10^{-5} obtained in conventional near-resonant optical lattices by more than two orders of magnitude. Although other systems like Bose-Einstein condensates subjected to far-detuned light-shift potentials provide far higher phase-space densities to date, for atoms confined well within the Lamb-Dicke regime in a near-resonant optical lattice, the present observations are interesting in their own right, because they show the capacity of DOL's to hold atom samples at densities considerably higher than those possible in BOL's. In fact, we do not observe any density-induced temperature increase or collisional losses, indicating that we have not yet reached fundamental limits; i.e., improved technical equipment should permit even higher phase-space densities in DOL's.

Our 3D DOL is produced by a superposition of a 2D DOL in the xy plane and an additional circularly polarized 1D lattice parallel to the z axis [cf. Fig. 1(a)]. The 2D DOL is produced according to Ref. [13] as the superposition of two 1D standing waves: a $\sigma_+\sigma_-$ wave along the x axis and a lin $\perp$ lin wave along the y axis. In addition, a homogeneous magnetic field in the z direction is applied. The two standing waves are derived from the two branches of a folded Michelson interferometer, which lets us choose their time-phase difference (by means of a piezoactuated mirror) to be $\psi = 90°$, such that the total energy density is spatially constant [cf. Fig. 1(b)]. In this case the 2D light field can be decomposed into two polarization components π and σ with electric field vectors parallel and perpendicular to the homogeneous magnetic field, such that the intensity nodes of the π component coincide with the antinodes of the σ component and vice versa. The frequency of the 2D-light field is detuned by 10Γ to the blue side of the $5S_{1/2}, F=3 \rightarrow 5P_{1/2}, F'=3$ transition of the $D1$ line of ^{85}Rb at 794.98 nm ($\Gamma = 2\pi \times 5.72$ MHz=natural linewidth of the $D1$ line). The σ component provides periodic potential wells for the $m=0$ Zeeman level with potential minima occurring in the nodes. The π component cannot couple to $m=0$ atoms and serves to optically pump the atoms into this state. The role of the magnetic field is to lift the Zeeman degeneracy in order to quench additional undesired dark states that otherwise would arise for the σ component.

Unfortunately, because the $F=3 \rightarrow F'=3$ transition of the $D1$ line is not closed, within a fraction of a microsecond the entire atomic population is optically pumped into the $F=2$ hyperfine component of the ground state and thus ceases to interact with the lattice field. Nearly every second photon contributes to this population transfer. Unlike in the operation of magneto-optic traps using nearly closed-cycle transitions, we cannot afford a resonant repumping field here, because the large number of repumping photons would significantly disturb the degree of darkness and the cooling performance of the DOL. Instead we have implemented a second 2D DOL with analogous polarization geometry on the blue side of the $F=2 \rightarrow F'=2$ transition (detuning $\approx 3\Gamma$), by coupling a second beam propagating parallel to the first beam to better than 10^{-5} rad to the Michelson interferometer [cf. Fig. 1(b)]. We have taken care that both DOL's are commensurable in the sense that in the region, where the atoms are trapped, the nodes and antinodes of their π and σ components exactly coincide. This guarantees that the appropriate spatial correlation between optical pumping rates and the light-shift potentials, which is a prerequisite for efficient Sisyphus cooling cycles, is maintained not only within each lattice but also when optical pumping transfers atoms between the two lattices. The spatial extension over which this matching can be accomplished is determined by the spatial beat length $\Delta L = c/\delta\nu = 11.5$ cm, which corresponds to the frequency interval $\delta\nu = 2.6$ GHz between the two lattices; i.e., spatial phase matching can be arranged on the few percent level over the entire millimeter-sized atomic sample. Both lattices should display the same polarization pattern, which implies equal values of the time-phase differences for both lattices, and their positions relative to each other need to be properly adjusted. To satisfy these requirements, the lengths of the interferometer arms [paths $P \rightarrow M_1$ and $P \rightarrow M_2$ in Fig. 1(b)], their difference, and the distances between the atomic sample [A in Fig. 1(b)] and each of the retroreflecting mirrors [M_1 and M_2 in Fig. 1(b)] are adjusted to be multiples of ΔL.

Both lattices are derived from grating-stabilized diode lasers [20]. The lattice beams have e^{-2} diameters of about 5 mm and can be controlled with respect to their frequencies and intensities by acousto-optical modulators (AOM's). The path-length difference between the two interferometer arms is measured and servo-controlled by means of a diode laser

emitting at a frequency detuned by several nanometers from all resonances. An experimental cycle begins with the preparation of precooled atoms in the MOT which is typically loaded for 1.5 s from a decelerated thermal atomic beam. Then during a few milliseconds successively the repumping beams and the MOT cooling beams are extinguished, the MOT magnetic field is replaced by a homogeneous field of a few (typically 8) gauss, and both lattice fields are activated. The potential wells of our optical lattice are sufficiently deep to capture the atoms directly from the MOT without additional cooling steps being needed. In order to obtain information on relevant parameters like the density and temperature, fluorescence imaging is used. The atoms are irradiated with a short pulse of the MOT beams (cooling beams and repumping beams) during several hundred microseconds and the fluorescence is imaged on a charge-coupled device (CCD) camera. The imaging system is carefully calibrated in order to yield correct values of the total number of atoms observed. The Zeeman substructure and the polarization geometry of the MOT light field are accounted for by an effective excitation probability according to the considerations described in Ref. [21].

Before we discuss its 3D extension we briefly characterize the 2D DOL. We have performed temperature measurements of the atoms in the 2D DOL using a time-of-flight (TOF) method. The atoms are subjected to the lattice for an adjustable time period (typically 1 ms), and subsequently the lattice is shut off and the atoms may expand freely during several milliseconds before their density distribution is monitored. Our observations show that during a short period (on the order of a few 100 μs) the transverse temperature (i.e., in the xy plane) is cooled from the initial MOT temperature of 70 μK to 13 μK, while the temperature corresponding to the the z direction is increased to 544 μK. These results are obtained in the large magnetic field regime ($B=8$ G) and for a well depth $U\sim 220E_{rec}$. The corresponding harmonic vibrational frequency is $\omega_{vib}=2\pi\times 110$ kHz and the Lamb-Dicke factor, which indicates the degree of suppression of inelastic photon scattering for well-localized vibrational states [22,23], amounts to $\eta=\hbar\omega_{vib}/E_{rec}\approx 30$.

We may estimate the degree of darkness in the DOL by observing the expansion of the atomic sample while trapped in the lattice. In the xy plane which provides confinement, the size of the atomic cloud remains constant, whereas the size in the unconfined vertical direction grows rapidly. In Fig. 2 we show the time evolution of the vertical radius $\sigma_z(t)$ (z direction) of the atomic sample. The data observed agree well with a simple model based on the assumption of pure ballistic expansion according to $\sigma_z=\sqrt{\sigma_{z,0}^2+(2k_BT_z/M)(t-t_0)^2}$, where $\sigma_{z,0}$ denotes the initial sample radius and $T_z=602$ μK is the temperature in the z direction in the lattice (cf. dashed line in Fig. 2). This indicates that during an initial time interval, shorter than the time needed for the atoms to travel a distance comparable to the initial sample radius, atoms subjected to the lattice are heated with respect to the unconfined z direction from the initial temperature of the MOT of $T_{z,i}=70$ μK to $T_z=602$ μK. We conclude that this initial heating results from photon scattering connected to the initial cooling in the transverse directions. After the initially hot atoms are transversely cooled into nearly dark states, photon scattering and consequential heating in the z direction become very small. The temperature derived from the ballistic model in Fig. 2 exceeds the temperature observed by TOF measurements, in which the atoms have spent about 1 ms in the lattice, by only $\delta T=58$ μK. This shows that after the lattice has reached its steady state in the transverse directions, only little residual heating in the z direction occurs. The difference δT (which is acquired in about 9 ms) corresponds to a photon scattering rate of only 1.8×10^3 s^{-1} once the transverse steady state is reached. The total temperature increase in the z direction results from the scattering of approximately $n_{sc}=(T_{z,f}-T_{z,i})/T_{rec}\approx 1500$ photons. Accounting for the optical pumping time of 270 ns this takes about 400 μs. The final temperature $T_{z,f}$ corresponds to a mean velocity of about 35 cm/s, and thus the lifetime of the 2D DOL is limited to around 10 ms.

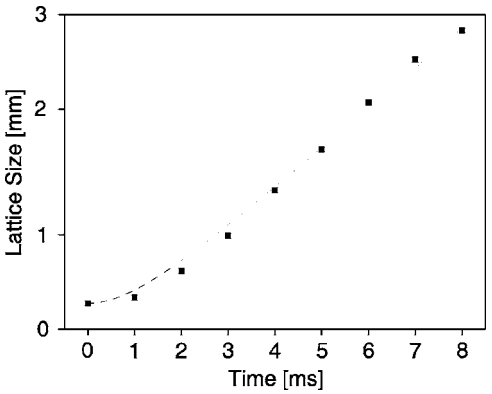

FIG. 2. Time evolution of the radius in the z direction of the atomic sample trapped in the 2D dark optical lattice. The dashed line illustrates the expectation for ballistic expansion with a temperature $T_z=602$ μK.

In order to understand the strategy for a 3D extension of the DOL recall that in the 2D DOL atoms in the $m=0$ Zeeman level are confined in the intensity nodes of the σ-polarization component which are arranged on lines parallel to the z axis. Thus, in order to add confinement in the z direction an additional σ-polarized standing wave extending along the z axis is required. Fortunately, if we employ circular polarization—e.g., σ_+—in contrast to the composition of the 2D lattice, we do not need to control the time phase of the third standing wave, because a change of this phase does not change the intensity distribution of the total σ component.

The additional confinement along the z axis leads to an increase of the lifetime. In the regime of large magnetic fields, where we typically operate our lattice, it attains values of around 120 ms, which, although being a more than a tenfold increase, still appears surprisingly short. If the magnetic field approaches zero—i.e., in the case of so-called dark optical molasses [24]—where the atoms are no longer confined in light-shift potentials, we observe a lifetime increase to much larger values of several seconds. This indicates the existence of a loss mechanism which is closely related to the existence of light-shift potentials. It seems that the prevailing

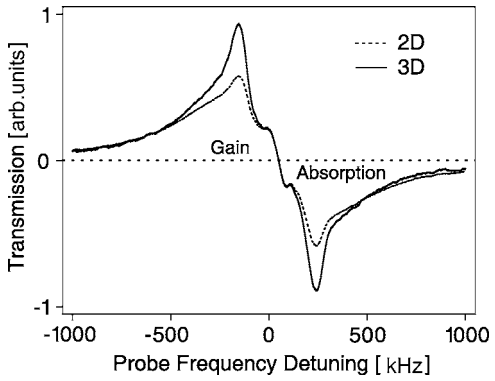

FIG. 3. Probe transmission spectra of 2D (dashed trace) and 3D (solid trace) dark optical lattices.

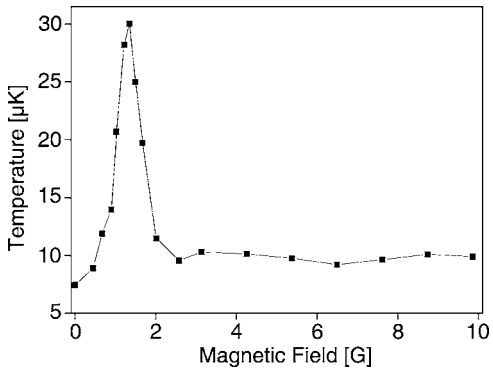

FIG. 4. The atomic kinetic temperature in the DOL (for $U \sim 700E_{rec}$) is plotted versus the static magnetic field. The atoms are subjected to the DOL for 6 ms before the temperature is measured by the TOF method. The solid line connects the data points to guide the eye.

cold fraction of atoms, localized deeply within the potential wells (about 90% of the atoms occupy the motional ground state), exchanges population with a small fraction of far more energetic atoms, which can readily propagate in the lattice and escape. We believe that this phenomenon is closely related to the fact that the blue frequency detuning used in DOL's produces Doppler heating for the small fraction of atoms at velocities exceeding the capture velocity of the Sisyphus mechanism. For small magnetic fields the potential well connected to the nearly dark state becomes increasingly shallow and the nearly dark state develops into a true dark state with a population approaching 100%. This explains the much increased lifetimes observed in this case. We do not observe losses due to collision processes, despite the relatively high densities in our DOL. This is in accordance with theoretical expectations [25], indicating that collisional loss is suppressed by the effects of the lattice potential and of optical shielding.

The lifetime increase observed for the 3D extension of the DOL together with a reduction of the temperature by nearly a factor of 3 (for comparable well depths) is also reflected by the probe transmission spectra shown in Fig. 3. Such spectra display pronounced resonances resulting from stimulated Raman transitions between adjacent vibrational modes in the potential wells and thus provide information on the degree of atomic confinement. Experimentally, a weak probe beam is sent through the atomic sample and its frequency is tuned across the frequency of the DOL [4]. In our experiment, the probe beam propagates within the xy plane and thus is sensitive only to vibrations within this plane. As seen in Fig. 3, in the 3D case the fraction of atoms contributing to the Raman peaks is significantly increased, indicating a temperature decrease. The overall signal size is also increased due to the increased lifetime. Probe transmission spectra are typically derived in 2 ms; i.e., they are useful as a real-time monitor for adjustment of the correct time-phase relation in the 2D DOL by maximizing the Raman peaks.

The temperature in the 3D DOL is observed to be uniform with respect to the x, y, and z directions and displays a significant dependence on the magnetic field strength B, which is shown in Fig. 4. The temperature takes its minimal value for $B=0$ and increases with the magnetic field in the range where the Zeeman splitting between the outermost ground state Zeeman sublevels is smaller than the average light shift of the coupled states. The temperature reaches its maximum when the Zeeman splitting is on the order of the average light shift and decreases towards an asymptotic value for larger values of B. These results resemble those obtained for cesium atoms in Refs. [19,26], and the physical interpretations found there apply here as well. However, as a significant difference to our work here, these experiments use a beam configuration, which does not provide true 3D confinement for $B>0$ but rather an antidotlike potential. For $B=0$, where independent of the light field configuration no confinement arises, we observe temperatures around 7 μK for deep potential wells $U \sim 700E_{rec}$ and 2 μK for shallow potential wells $U \sim 75E_{rec}$. In the high-magnetic-field regime, where our DOL provides Lamb-Dicke confinement in all spatial directions, the temperatures are about a factor of 1.5 larger. This behavior is similar to that observed in [19] (although our temperatures are generally slightly lower despite the increased confinement), but in contrast to the theoretical results of Ref. [26] which predict an order of magnitude temperature increase, when the high-magnetic-field regime is approached.

The Sisyphus cooling mechanism in the regime of large magnetic fields resembles that observed in BOL's. The eigenstates of the system are nearly identical with the Zeeman sublevels and the light shift acts as a perturbation that gives rise to a spatial modulation of the eigenenergies. In this limit, the depth of the potential wells and, hence, the temperature of the atoms are approximately proportional to the light intensity and nearly independent of the magnetic field. This is confirmed in Fig. 5, where the kinetic temperature is plotted versus the light intensity for a magnetic field of $B=8$ G, well within the high-magnetic-field regime. We also plotted the corresponding population of the vibrational ground state (derived within the harmonic approximation) which for well depths above $75E_{rec}$ attains remarkably high values of around 90%. Hence, in the regime of large magnetic fields the temperature of the lattice is mainly determined by the quantum-mechanical momentum spread of the motional ground state. For $U \sim 75E_{rec}$ we observe minimal temperatures around 2.8 μK which corresponds to $\sim 7.8T_{rec}$. This is an order of magnitude below the minimal temperatures pre-

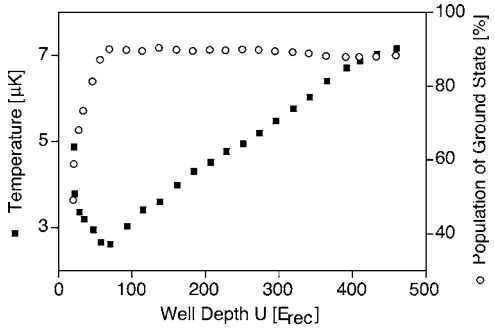

FIG. 5. The kinetic temperature (solid rectangles) and the population of the vibrational ground state (open circles) in the DOL are plotted versus the well depth U in the high-magnetic-field regime ($B=8$ G). The intensities of the lattice beams acting upon the $F=2\rightarrow F'=2$ and $F=3\rightarrow F'=3$ transitions are proportionally varied. The plotted quantities correspond to the $F=3\rightarrow F'=3$ lattice. The atoms interacted with the lattice for 15 ms.

dicted in Ref. [26] for large B values. We attribute these low temperatures to the spatially phase-matched, bichromatic geometry of our DOL, which prevents heating contributions due to optical hyperfine pumping. Approaching zero intensity we recognize the known *décrochage* behavior typical for Sisyphus cooling [14,28].

In oder to increase the occupation of the DOL we have added the FOL as illustrated in Fig. 1(a). The FOL results from a linearly polarized vertically oriented [z axis in Fig. 1(a)] standing wave, derived from a diode laser which injects a tapered amplifier, thus providing 180 mW usable light power. Its frequency is tuned to 182 GHz below the $3S_{1/2}\rightarrow 3P_{3/2}, F=3\rightarrow F'=4$ resonance at 780.24 nm, and its intensity can be controlled by an AOM. The limited available power restricted us to a relatively shallow trap of 173 μK with corresponding axial and radial harmonic frequencies of 236 kHz and 166 Hz, respectively, and a moderate e^{-2} trap radius of 250 μm. Because our scheme for increasing the density relies on knowing the prevailing radial oscillation frequency of the atoms and since the calculated value relies on the harmonic approximation, we determined this parameter experimentally by introducing resonant parametric heating [27]. The trap depth was modulated with a step function

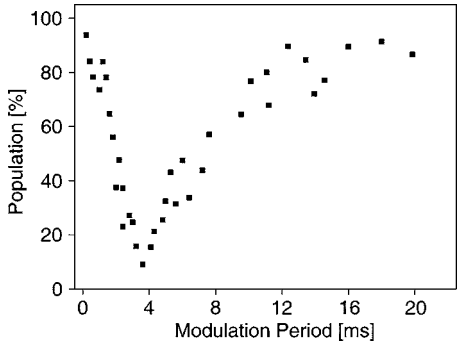

FIG. 6. Determination of the radial oscillation frequency in the FOL by parametric heating. The trap depth was modulated with a step function with a variable time period plotted on the x axis, while the fraction of atoms remaining trapped after 30 ms is recorded on the y axis.

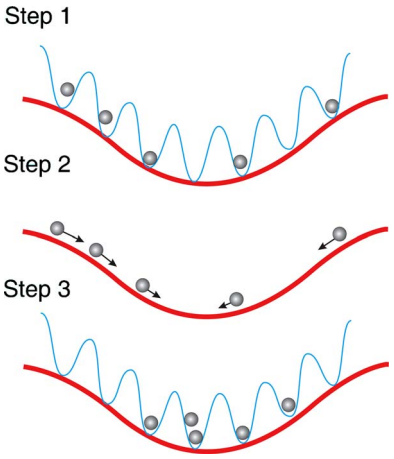

FIG. 7. (Color online) Scheme for the density enhancement in the FOL via parametrical modulation of the three-dimensional dark optical lattice.

with 8% contrast and variable time period, and the number of atoms remaining trapped after 30 ms was measured. According to the observations in Fig. 6 the maximum heating occurred at a period of $\tau_{max}=3.4$ ms; i.e., an oscillation frequency $\nu_{osc}=1/2\tau_{max}=147$ Hz is found. This value is slightly lower than the the prediction of the harmonic approximation, showing that the atoms extend into the nonharmonic regions of the potential wells.

Our scheme to increase the density is inspired by previous work with cesium atoms [15]. We apply alternating cycles of cooling in the DOL and synchronized oscillations in the FOL. The FOL provides nearly harmonic potential wells such that after a quarter of the atomic oscillation time a compression of the atoms arises which is frozen by the reactivated DOL. We proceed in three steps sketched in Fig. 7.

(i) The first step (cf. Fig. 7, step 1) begins with the preparation of 2×10^9 rubidium atoms in the MOT with 70 μK temperature and a density of 5×10^{10} atoms/cm^3. The FOL is activated and a fraction of about 5×10^7 atoms is loaded into the FOL. The MOT is extinguished, and after a time delay of 30 ms, which serves to remove atoms, not captured in the FOL, by gravity,[1] the DOL is activated and the atoms are cooled into the microscopic light-shift potentials of the DOL at typical densities of 3×10^{11} atoms/cm^3 and temperatures around 10 μK.

(ii) In the second step (cf. Fig. 7, step 2), the well depth of the DOL is adiabatically reduced 1000-fold during $\tau_{2a}=400$ μs, which yields further cooling to temperatures around 3 μK, and finally switched off completely. The atoms are now subjected to the FOL potential wells only during a variable time τ_{2b}; i.e., they move dissipation free in an array of about 2500 horizontally oriented "pancake-shaped" microtraps arranged along the z axis at 390 nm mutual separation.

(iii) In the third step (Fig. 7, step 3), the DOL is reactivated during a time interval τ_3 in order to freeze the oscillatory motion of the atoms in the FOL and again cool them

[1]This step is necessary because these atoms represent the majority and may otherwise prevent the detection of the captured atoms.

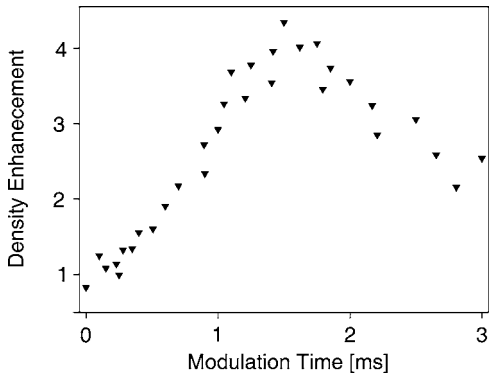

FIG. 8. The peak density is plotted versus the duration τ_{2b} of the free evolution in step 2 of our density increase procedure. The density is scaled to the value observed for $\tau_{2b}=0$.

into the microscopic light-shift potentials of the DOL to 10 μK.

In a typical experiment the latter two steps are repeated several times until the sequence ends with step 2 and a fluorescence image of the atoms is taken, which lets us determine the atom number and peak density. In Fig. 8, steps 2 and 3 are alternated during 10 ms with equal durations for steps 2 and 3—i.e., $\tau_{2a}+\tau_{2b}=\tau_3$. The observed peak density is plotted versus the duration τ_{2b} of the free evolution in step 2, finding a maximal peak density of 1.2×10^{12} atoms/cm^3 for $\tau_{2b}=1.6$ ms which represents a fourfold density increase as compared to the case when $\tau_{2b}=0$ ms. The observed value $\tau_{2b}=1.6$ ms falls within the two values of a quarter of the oscillation time, calculated in the harmonic regime to be 1.5 ms and measured by parametric heating in Fig. 6 to be 1.7 ms.

The density increase in Fig. 8 displays a relatively broad resonance behavior, indicating that we do not operate well within the harmonic regime of the FOL, such that a broad spectrum of oscillation frequencies arises. A larger-sized FOL could definitely yield much improved results. Technically, we are limited by the power from our FOL laser source. A second, even more dramatic technical deficiency of our laser source is its spectral impurity resulting from the fluorescence background of the tapered amplifier used. The near-resonant spectral components of this background introduce excess photon scattering and light-induced losses which has limited the lifetime of our FOL to about 80 ms. Since the duration of our experimental procedures is comparable to this time, we typically lose half of the atomic population. We estimate that with 1 W of spectrally clean radiation—e.g., from a titanium-sapphire laser—a fourfold improvement of our results should be expected. We have no indications that at the density level reached here light-induced interactions act as a limiting factor, which for comparable conditions would be a serious limitation in bright optical lattices. After the compression procedure, we can keep the atoms trapped in the 3D DOL without additional density-dependent losses or heating observed.

In summary, we have studied a bichromatic dark optical lattice of rubidium atoms, providing confinement in the Lamb-Dicke regime in all spatial dimensions. A novel kind of lattice geometry permits Sisyphus cooling cycles undisturbed by optical hyperfine pumping, yielding improved performance with regard to temperature and vibrational ground-state occupation. We have explored a compression scheme to increase the fraction of occupied lattice sites. Limited only by technical deficiencies of one of our laser sources, we obtain 7.5% occupation and a temperature of 2.8 μK, which corresponds to a phase-space density of 1.7×10^{-3}. This represents an improvement by more than two orders of magnitude as compared to typical phase-space densities of 10^{-5} obtained in conventional near-resonant optical lattices. A further increase of the phase-space density by a factor of 4 appears possible with simple technical improvements. It should be interesting to investigate optical shielding [25] in near-resonant dark optical lattices with increased occupation.

This work has been supported by the Deutsche Forschungsgemeinschaft (DFG) under Contract No. He2334/2-1.

[1] *Coherent and Collective Interactions of Particles and Radiation Beams*, Proceedings of the International School of Physics "Enrico Fermi," Course CXXXI, Varenna, 1995, edited by A. Aspect, W. Barletta, and R. Bonifacio (IOS, Amsterdam 1996).
[2] P. Jessen and I. H. Deutsch, Adv. At., Mol., Opt. Phys. **37**, 95 (1996).
[3] L. Guidoni and P. Verkerk, J. Opt. B: Quantum Semiclassical Opt. **1**, R23 (1999).
[4] G. Grynberg and C. Robilliard, Phys. Rep. **355**, 335 (2001).
[5] T. Walker *et al.*, Phys. Rev. Lett. **64**, 408 (1990).
[6] D. Sesko *et al.*, J. Opt. Soc. Am. B **8**, 946 (1991).
[7] A. Hemmerich *et al.*, Europhys. Lett. **21**, 445 (1993).
[8] D. Sesko *et al.*, Phys. Rev. Lett. **63**, 961 (1989).
[9] F. Dalfovo *et al.*, Rev. Mod. Phys. **71**, 463 (1999).
[10] D. Jaksch *et al.*, Phys. Rev. Lett. **81**, 3108 (1998).
[11] M. Greiner *et al.*, Nature (London) **419**, 51 (2002).
[12] G. Grynberg and J.-Y. Cortois, Europhys. Lett. **27**, 41 (1994).
[13] A. Hemmerich *et al.*, Phys. Rev. Lett. **75**, 37 (1995).
[14] G. Dalibard and C. Cohen-Tannoudji, J. Opt. Soc. Am. B **6**, 2023 (1989).
[15] T. Marshall *et al.*, Phys. Rev. Lett. **82**, 2262 (1999).
[16] E. L. Raab *et al.*, Phys. Rev. Lett. **59**, 2631 (1987).
[17] C. S. Adams and E. Riis, Prog. Quantum Electron. **21**, 1 (1997).
[18] K. I. Petsas *et al.*, Europhys. Lett. **46**, 18 (1996).
[19] C. Triché *et al.*, Opt. Commun. **126**, 49 (1996).
[20] L. Ricci *et al.*, Opt. Commun. **117**, 541 (1995).
[21] C. Townsend *et al.*, Phys. Rev. A **52**, 1423 (1995).
[22] J.-Y. Courtois and G. Grynberg, Phys. Rev. A **46**, 7060 (1992).
[23] P. Jessen *et al.*, Phys. Rev. Lett. **69**, 49 (1992).
[24] D. Boiron *et al.*, Phys. Rev. A **53**, R3734 (1996).
[25] J. Piilo and K.-A. Suominen, Phys. Rev. A **66**, 013401 (2002).
[26] K. I. Petsas *et al.*, Phys. Rev. A **53**, 2533 (1996).
[27] T. Savard *et al.*, Phys. Rev. A **56**, R1095 (1997).
[28] J. Jersblad *et al.*, Phys. Rev. A **62**, 051401(R) (2000).